Neuropsychopharmacology (2011) 36, 1792–1800

www.neuropsychopharmacology.org

The Effects of Nicotine Replacement on Cognitive Brain Activity During Smoking Withdrawal Studied with Simultaneous fMRI/EEG

John D Beaver*[,1], Christopher J Long[1], David M Cole[1,2], Michael J Durcan[3], Linda C Bannon[3], Rajesh G Mishra[3] and Paul M Matthews[1,2]

[1]GlaxoSmithKline Clinical Imaging Centre, Hammersmith Hospital, London, UK; [2]Department of Clinical Neuroscience, Imperial College, London, UK; [3]GlaxoSmithKline Consumer Healthcare, Weybridge, UK

Impaired attention ('difficulty concentrating') is a cognitive symptom of nicotine withdrawal that may be an important contributor to smoking relapse. However, the neurobiological basis of this effect and the potentially beneficial effects of nicotine replacement therapy both remain unclear. We used functional MRI with simultaneous electroencephalogram (EEG) recording to define brain activity correlates of cognitive impairment with short-term smoking cessation in habitual smokers and the effects of nicotine replacement. We found that irrespective of treatment (ie nicotine or placebo) EEG α power was negatively correlated with increased activation during performance of a rapid visual information processing (RVIP) task in dorsolateral prefrontal, dorsal anterior cingulate, parietal, and insular cortices, as well as, caudate, and thalamus. Relative to placebo, nicotine replacement further increased the α-correlated activation across these regions. We also found that EEG α power was negatively correlated with RVIP-induced deactivation in regions comprising the 'default mode' network (ie angular gyrus, cuneus, precuneus, posterior cingulate, and ventromedial prefrontal cortex). These α-correlated deactivations were further reduced by nicotine. These findings confirm that effects of nicotine on cognition during short-term smoking cessation occur with modulation of neuronal sources common to the generation of both the blood oxygen-level-dependent and α EEG signals. Our observations thus demonstrate that nicotine replacement in smokers has direct pharmacological effects on brain neuronal activity modulating cognitive networks.
Neuropsychopharmacology (2011) **36,** 1792–1800; doi:10.1038/npp.2011.53; published online 4 May 2011

Keywords: nicotine; cognitive impairment; smoking; addiction; fMRI; EEG

INTRODUCTION

Over 1 billion people currently smoke tobacco and half of all long-term smokers die from smoking-related illnesses (Royal College of Physicians, 2007). However, nicotine dependence is difficult to treat. Only 5–7% of unassisted attempts to stop smoking are successful for >6 months; multiple attempts typically are necessary to achieve long-term abstinence (Hughes *et al*, 2008). Mild cognitive impairments such as difficulty concentrating are an established symptom of nicotine withdrawal, and may be an important trigger for smoking relapses (Parrott and Roberts, 1991; Parrott *et al*, 1996). Furthermore, anticipation of these symptoms adds to the challenge of initiating repeat attempts at cessation. Previous research has demonstrated that nicotine replacement is effective in reversing withdrawal-induced performance deficits on cognitive tests of sustained attention and working memory (Atzori *et al*, 2008). However, the specific pharmacodynamic mechanisms of nicotine responsible for this clinically important treatment effect have not been defined.

Functional magnetic resonance imaging (fMRI) of smokers suggests that nicotine replacement prior to the onset of withdrawal modulates brain activity during cognitive task performance in regions previously implicated in arousal, attention, and working memory. For example Lawrence *et al* (2002) showed that applying a nicotine patch to minimally abstinent smokers results in increased blood oxygen-level-dependent (BOLD) signal in the parietal cortex, caudate, and thalamus during performance of a rapid visual information processing (RVIP) task, and reduced BOLD response in parahippocampal gyrus and insula. More recent fMRI studies of nicotine replacement

*Correspondence: Dr JD Beaver, GlaxoSmithKline Clinical Imaging Centre, Hammersmith Hospital, Du Cane Road, London W12 0NN, UK, Tel: +44 20 8008 6014, Fax: +44 20 8008 6491,
E-mail: j.beaver@cantab.net
Received 19 April 2010; revised 25 February 2011; accepted 25 February 2011

prior to withdrawal onset have shown that nicotine replacement is also associated with decreased BOLD response in regions of the so-called 'default mode' network and thalamus (Hahn *et al*, 2007, 2009). However, whether nicotine replacement following withdrawal onset changes cognitive brain activity was not made clear by these initial studies.

In addition, functional MRI does not measure neuronal activity directly, but is based on the interaction between vascular responses and local tissue oxidative metabolism (Ogawa *et al*, 1990). A critical concern for all pharmacological fMRI studies is the possibility that BOLD responses may be induced by non-neuronal drug effects (eg, alterations in neurovascular coupling), rather than drug-induced changes in neuronal activity (Iannetti and Wise, 2007; Matthews *et al*, 2006). This may be particularly important for studies of agents like nicotine, which can have direct pharmacological effects on cerebral vasculature (Iida *et al*, 1998). Several previous fMRI studies of nicotine's effects on cognition have attempted to address this issue by demonstrating the absence of treatment effects on resting cerebral blood flow (as assessed with arterial spin labeling) and regional BOLD signal during a control activation task (Hahn *et al*, 2007, 2009).

To assess brain activity related to cognitive enhancement by nicotine replacement in withdrawal, we used BOLD fMRI with simultaneous electroencephalographic (EEG) recording while abstinent smokers performed an RVIP task. Integration of the EEG, which provides a direct electrophysiological measure of neuronal activity, with fMRI increased confidence that signals measured with the latter reflected true neuronal responses. Prior to each fMRI scan, participants were deprived of cigarettes for 8 h before being dosed with nicotine or placebo lozenges in a double-blind, crossover design. We hypothesized that task-related modulation of the BOLD signal would be inversely correlated with EEG α power in brain regions previously implicated in sustained attention, executive function, and working memory, as well as regions of the default network. We further hypothesized that (relative to placebo) nicotine replacement during smoking withdrawal would potentiate the α-correlated BOLD activity in each of these regions.

MATERIALS AND METHODS

Participants

We enrolled 23 right-handed, adult smokers, with no history of neurological/psychiatric illness (confirmed in writing by their GP) or current drug use (other than tobacco smoking). Participants smoked regularly for at least 3 years, smoked an average of 15 commercially available cigarettes per day, and normally consumed a cigarette within 30 min of waking. Data from eight participants did not pass both fMRI and EEG quality control checks (see Data analysis), and, therefore, all data from these subjects were excluded from analysis. For the final pool of 15 participants (four females; mean age = 30.3 years ± 7.7 (SD), range = 21–49 years), scores on the Fagerström test for nicotine dependence (Heatherton *et al*, 1991) were 5.1 ± 1.5 (mean ± SD). All participants gave written, informed consent and the protocol was approved by the Charing Cross Hospital Research Ethics Committee, London, UK.

Study Design

Each participant underwent screening followed by two treatment visits in a randomized, placebo-controlled, crossover design with at least 48 h between treatment visits. Participants received either 4 mg nicotine lozenges (NiQuitin CQ, GlaxoSmithKline), or taste-matched placebo lozenges containing capsicum at each visit.

A detailed sequence of events at each treatment visit is presented in Supplementary Table 1. At each visit, participants arrived at the clinic at approximately 06:30 hours. Under supervision, participants smoked one cigarette and then abstained from smoking for 8 h before the first dosing and thereafter until the end of the session. Subjects completed a computerized RVIP task ~60 min prior to the first-dose administration to minimize possible practice effects. This task was administered inside the scanner while it was not active to acclimatize volunteers to the scanning environment prior to actual data collection. Subjects were subsequently dosed with either the 4-mg nicotine lozenge or placebo at time 0 and then again after 2 h. Previous behavioral studies in smokers have shown that the 4-mg nicotine lozenge dosed in this way significantly improves withdrawal-induced performance deficits on an RVIP task (Atzori *et al*, 2008). Immediately prior to both dose administrations, subjects were asked to complete subjective ratings of nicotine withdrawal and cigarette craving using the Modified Minnesota Withdrawal Symptom (MMWS) scale (Hughes and Hatsukami, 1986; Heatherton *et al*, 1991). Simultaneous fMRI/EEG data acquisition during performance of the computerized RVIP task began ~60 min following the final dosing, and lasted for ~28 min. After being removed from the MR scanner, subjects again completed subjective ratings of nicotine withdrawal and cigarette craving using the MMWS.

Cognitive Task

The cognitive task consisted of a series of centrally displayed, single numbers (0–9) back projected into the bore of the scanner at a rate of 100 per minute. During RVIP blocks, participants identified sequences of three consecutive odd or even numbers from a pseudo-random sequence by pressing the corresponding button on a response box as quickly as possible. During control (CNTRL) blocks, participants identified single occurrences of the number '0.' The number and position of targets within each block were matched and counterbalanced across block type. Each block lasted 90 s and there were eight blocks of each type in total, presented in counterbalanced order. A 30-s rest block was presented after every two consecutive blocks during which participants were instructed to fixate a centrally displayed (+) symbol. The dependent variables were accuracy (number of correctly identified targets/total number of targets) and response time (the average response time in milliseconds to correctly identify targets).

fMRI Acquisition

At each visit, single-shot, T2*-weighted, gradient-echo planar imaging (EPI) sensitive to BOLD contrast was carried out during performance of the task on a 3-Tesla MAGNETOM TIM Trio whole-body MRI scanner (Siemens, Erlangen, Germany) with a 12-channel birdcage radio-frequency head coil. Images were collected in one continuous run of 548 volumes. Whole-brain images were acquired in 41 slices (TR = 3000 ms, TE = 30 ms, flip angle = 90°, voxel size = 3.5 mm isotropic). The first four volumes were discarded to allow for magnetic equilibration. Additional high-resolution T1-weighted anatomical MRI scans (MPRAGE) were acquired for each subject to aid with EPI co-registration (TR = 3000 ms, TE = 3.66 ms, flip angle = 9°, voxel size = 1 mm isotropic, 208 slices).

EEG Acquisition

EEG was continuously recorded inside the MRI scanner during task performance using the MRI-compatible BrainAmp system (Brainproducts, GmbH, Germany). We recorded from 32 scalp sites positioned according to 10–20 system (including channels O_1, O_2, P_3, P_4 used in α analyses) with the average of mastoid channels TP_1 and TP_2 used as a reference node. The 'BrainCap' (BrainProducts) MRI-compatible sintered Ag/AgCl ring electrodes were placed in contact with the scalp using MR-compatible conductive electrolyte gel around the electrodes. Electrode impedance was kept below 10 KΩ. An electrode was placed on the infra-orbital ridge of the right eye to record vertical EOG. The BrainProducts BrainAmp ExG system was used to measure high SNR bipolar electrocardiograms (ECGs) to capture cardiac dynamics. All data (EEG and ECG) were digitized through amplifiers with the following specifications: 1000 Hz low-pass filter, 10 s (time constant) high-pass filter, with a 5000-Hz sampling rate and a 16-Bit analog to digital quantization resolution featuring a dynamic range of ± 600 mV. The EEG amplifier was placed directly behind the head coil inside the scanner bore, and connected by fiber optic to the recording and analysis computer located in the control room. The ECG amplifier was placed at the foot of the scanner with the cables routed to be approximately parallel to the system Gauss lines, avoiding the head coil entirely. Both amplifiers were weighted with sandbags to mitigate the effects of gradient-induced vibration. We synchronized the EEG amplifier clock with the 10-MHz master clock of the TIM Trio system to record EEG and ECG in phase with MRI gradient switching.

Data Analysis

EEG preprocessing. We used Brain Vision Analyzer (Brainproducts) to perform off-line correction of gradient imaging and ECG artefacts as described previously (Allen *et al*, 1998, 2000). A detailed description of our EEG preprocessing procedure is provided in Supplementary Information. The EEG data were manually inspected to assess the efficacy of the preprocessing. Data from eight participants were discarded due to significant corruption of >20% of the EEG or failure to successfully remove artefacts. For the remaining 15 subjects, we derived α power time courses by computing the power spectral density (PSD) using a fast Fourier transform with a windowing width corresponding to the fMRI TR (3 s). The spectral α power was derived for each TR by integrating the PSD within the α frequency band (~8–12 Hz).

fMRI preprocessing. fMRI data were analyzed with FSL version 4.1 (http://www.fmrib.ox.ac.uk/fsl/). Individual sessions with mean head motion exceeding the in-plane size of a voxel (3 mm) were excluded (incidentally, these sessions were restricted to subjects who were discarded due to poor quality EEG data). Data were high-pass filtered, spatially smoothed (6 mm full width half maximum Gaussian kernel), and corrected for motion using a rigid-body transformation to align each image in the series with the mid-image of the run. Further preprocessing included grand mean intensity normalization of the entire 4D data set by a single scaling factor.

Integration of EEG and fMRI data. The approach we used here attempts to build on earlier correlation approaches originally utilized to explore the relationship between EEG α power time courses and BOLD signals at rest (Laufs *et al*, 2003). In general, a correlation score computed between two signals reflect only temporal synchronicity, independent of possible changes in amplitude. We, therefore, employed a regression-based model to capture both synchronicity and amplitude. Sensitivity to amplitude is critical to our present work because we employed a cognitive task designed to experimentally manipulate the signal amplitude. This approach also contrasts with previous investigations that examined correlative EEG/fMRI relationships on subjects at rest.

Building upon standard fMRI time-series approaches (Smith, 2004), we combined the estimated EEG α power dynamics with empirical observations about the nature and form of the fMRI noise $w_{t,v}$ culminating in the following model for the time course at each location in the brain. That is, we used the model $x_{t,v} = m_v + s_{t,v}^{\mathrm{Alpha}} + w_{t,v}$ to integrate EEG α signal with fMRI data at each voxel, v, in the brain, where m_v is the signal mean and the observed time courses have been treated for low-frequency nuisance effects by a weighted running lines smoother (Woolrich *et al*, 2009). $w_{t,v}$ was a serially correlated first-order autoregressive stochastic noise component present to capture physiological fluctuations in the data not related to the task design. Since we operate on the assumption that EEG α power directly correlates with the fMRI BOLD signal (Laufs *et al*, 2003), we can decouple the α signal $s_{t,v}$ into two components: (a) a steady state or mean signal to capture the task design, c_t, and (b) residual amplitude fluctuations in the brain response reflected by changes in the α power curve. We decomposed $s_{t,v}^{\mathrm{Alpha}}$ into its task-related (constant) component and the EEG-derived variations about this constant component as follows: $s_{t,v}^{\mathrm{Alpha}} = \bar{s}_{t,v} + \tilde{s}_{t,v}$ (see Supplementary Figure 2), with the steady-state component of the EEG proportional to the standard fMRI block response $\bar{s}_{t,v} = H(t - D_v)\left(g_{v,t} * c_{t-D_v}\right)$ D_v was a hemodynamic delay of 6 s and H was a Heaviside step function. The hemodynamic response $g_{v,t}$ was characterized by a discrete γ function with a dispersion constant (sd = 3 s). Next, we computed the α power fluctuation $\tilde{s}_{\cdot,v}$ about the steady state

$\bar{s}_{\cdot,v}$ by fitting the observed α power curve $s_{t,v}^{\text{Alpha}}$ onto the fMRI model such that $\bar{s}_{\cdot,v} \perp \tilde{s}_{\cdot,v}$. Specifically these power fluctuations can be computed as the residuals of the fitted linear model, $\tilde{s}_{t,v} = s_{t,v}^{\text{Alpha}} - \gamma \bar{s}_{t,v}$, where the scaling factor γ is derived as a natural by-product of this linear model-based orthogonalization. That is, $\gamma = \sum_t \left(\bar{s}_{t,v} \cdot s_{t,v}^{\text{Alpha}}\right) / \sum_t \left(\bar{s}_{t,v} \cdot \bar{s}_{t,v}\right)$ This computation was performed at the start of the analysis of each session and subsequently fit at each fMRI voxel with spatially fixed γ and $\tilde{s}_{t,v}$ but with spatially varying estimates of the constant model BOLD response amplitudes, alongside the α power rhythm amplitudes. In summary, this approach simultaneously models amplitude fluctuations in the fMRI data related to underlying α activity that complements estimations related to the steady-state fMRI time-series model fit. More information on the rationale behind this approach is presented in Supplementary Information.

Statistical analysis of fMRI/EEG data. We estimated the signal parameters at each voxel using a weighted least squares model with intrinsic correction for spatial autocorrelations (Woolrich *et al*, 2009). Experimental regressors consisted of task condition using a blocked design matrix with one column assigned to each condition (RVIP or CNTRL). Each of these columns was convolved with a predefined hemodynamic response function to imputed lag and response of the brain function to the stimulus intrinsic to the system dynamics of the neurovascular response. An additional column incorporated the orthogonalized EEG α power time series. The nuisance part of the design matrix was configured to model head motion (values derived from the initial motion correction stage), and behavioral response times to control for potential effects of nicotine on the speed of processing. Each individual statistical map was normalized into a standard reference space (the MNI-152 template) using the FMRIB linear image registration tool for comparison across individuals. At the individual level, *Z*-statistic images were thresholded at cluster significance threshold of $P<0.05$ (whole-brain corrected for multiple comparisons).

Group mixed-effects analyses were then performed to produce *Z* (Gaussianized T/F) statistic images corrected for multiple comparisons using Gaussian Random Field Theory-based maximum height thresholding, with a corrected significance threshold of $P<0.005$. In all figures, activation maps are shown overlaid on the MNI-152 high-resolution image. To test the effects of nicotine on task-related activity, we created functionally defined regions of interest (ROIs) for the contrast RVIP–CNTRL (rest periods were not analyzed). In task-related regions specified in this way, we recorded for the task conditions, in each region, and each subject, the mean percent BOLD change within the mask. This procedure simplified the data analysis by overall reduction of the magnitude of the multiple testing problems of whole-brain approaches, while allowing for inter-subject variability in the exact area of activation (while still constraining each ROI's response to a specific mask).

Functionally defined ROI masks may potentially bias the resulting inferences unless the contrast generating the masks is statistically independent from the contrast of interest. Therefore, we ensured independence by computing initial ROI masks based on a mixed-effects group analysis collapsed across both visits (ie by accounting for the nicotine and placebo treatment effect in the mixed-effects statistical model). This two-dose average is, therefore, independent to our main comparison of interest (ie, nicotine *vs* placebo), and hence did, not bias our results.

The statistical maps were divided into anatomical regions using the Harvard–Oxford atlas (Harvard Center for Morphometric Analysis) to label and constrain clusters of activated voxels to anatomical regions. These ROIs were then applied to each individual subject's fMRI data and the mean regional percent BOLD signal change was extracted during task performance on each dosing visit. For the main contrasts of interest (RVIP–CNTRL), we assessed significance by using a corrected maximum height α-level of 0.005.

RESULTS

Behavioral Measures

Nicotine withdrawal was assessed using the MMWS scale once prior to dosing and again immediately after the fMRI scan. The post-dose assessment corresponded to 1.75 h ($\pm$30 min) after the second dose and 11.75 h ($\pm$30 min) after the subject's last cigarette. The mean pre-dose MMWS scores were 8.0 ($\pm$1.02 SE) and 8.5 ($\pm$0.78 SE) for the nicotine and placebo visits, respectively ($t(14) < 1$, NS). Paired *t*-test of the post-dose MMWS scores showed that the subjective experience of withdrawal was significantly lower following nicotine lozenge relative to placebo ($t(14) = 2.43$, $P<0.02$) (Figure 1). There was also a significant effect of nicotine on RVIP accuracy, with significantly greater accuracy following nicotine compared with placebo ($t(14) = 2.61$, $P<0.02$; Figure 2). Furthermore, response times to correctly identify target RVIP sequences were significantly faster for nicotine compared with placebo ($t(14) = 3.33$, $P<0.005$; Figure 2). We did not find a significant difference in accuracy between nicotine and placebo visits for the control task ($t<1$), but there was a near-significant trend toward faster response times following nicotine ($t(14) = 3.33$, $P = 0.0512$). This was expected because the control task was designed to place low attentional/cognitive demands on participants, resulting in so-called 'ceiling effects' in which participants perform

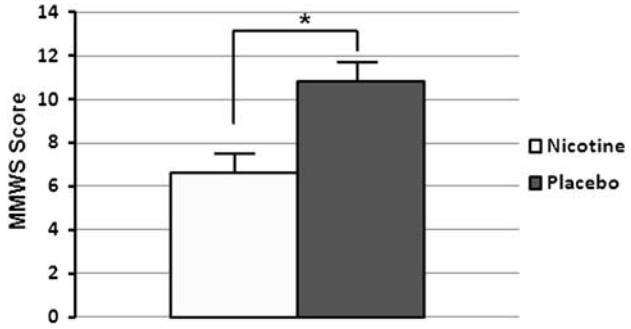

Figure 1 Effects of nicotine on subjective experience of withdrawal. Mean scores (+SEM) from the Modified Minnesota Withdrawal Symptom (MMWS) questionnaire administered immediately after scanning ($N = 15$, $^*P<0.05$).

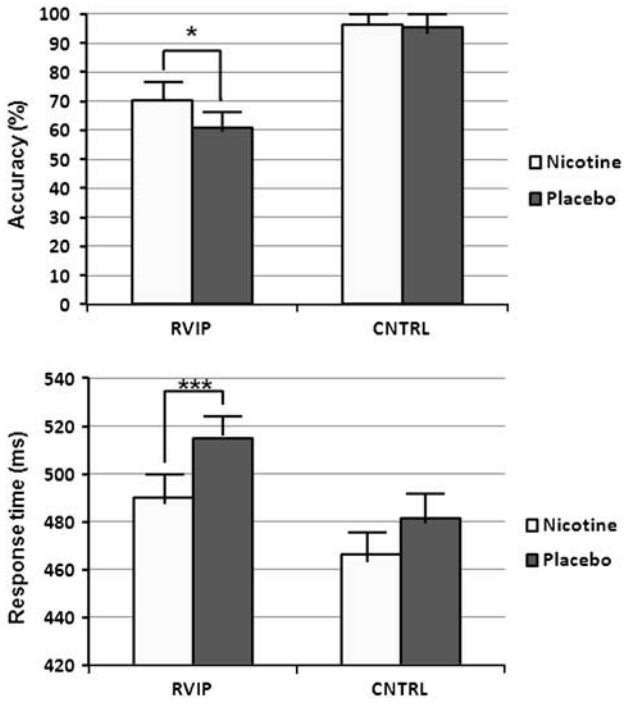

Figure 2 Effects of nicotine on behavioral measures of task performance. (Top panel) Mean (+SEM) percentage of correctly identified targets. (Bottom panel) Mean (+SEM) response time (in ms) to correctly identify targets. ($N = 15$, $^{*}P < 0.05$; $^{***}P < 0.001$).

very well irrespective of treatment with little room for improvement.

EEG α

We fit the processed α time-course data to the task model (as shown in Supplementary Figure 1) for each subject and session to compute the mean α PSD during RVIP performance. Paired *t*-tests confirmed that the mean α power during RVIP was significantly attenuated following nicotine replacement compared with placebo ($t(14) = -1.77$, $P < 0.05$).

Combined fMRI/EEG Data

Identification of RVIP-related activity. For the contrast RVIP–CNTRL collapsed across both treatment sessions, we identified six regions showing significant *increased* activation negatively correlated with EEG α power. Regions of significant increased activation included the bilateral caudate ($X_{max} = -10$, $Y_{max} = -2$, $Z_{max} = 10$, $z_{max} = 6.091$, nVOX = 75), dorsal anterior cingulate cortex ($X_{max} = 8$, $Y_{max} = 18$, $Z_{max} = 36$, $z_{max} = 10.62$, nVOX = 552), dorsolateral prefrontal cortex ($X_{max} = -44$, $Y_{max} = 6$, $Z_{max} = 34$, $z_{max} = 14.47$, nVOX = 2860), insula ($X_{max} = -34$, $Y_{max} = 18$, $Z_{max} = 0$, $z_{max} = 9.649$, nVOX = 332), parietal lobule ($X_{max} = 24$, $Y_{max} = -58$, $Z_{max} = 42$, $z_{max} = 14.11$, nVOX = 3379), and thalamus ($X_{max} = -8$, $Y_{max} = -16$, $Z_{max} = 6$, $z_{max} = 8.845$, nVOX = 249) (Figure 3a). In each of these regions, *increased* BOLD response during performance of the RVIP task was associated with *reduced* α power. Supplementary Figure 3 presents an example time-course plot depicting the close correlation of the BOLD fMRI and α EEG signals in the dorsal anterior cingulate of a single participant.

We also identified five regions showing significant *decreased* activation (for the RVIP–CNTRL contrast) negatively correlated with α power. These regions included angular gyrus ($X_{max} = -42$, $Y_{max} = -68$, $Z_{max} = 22$, $z_{max} = -6.112$, nVOX = 1770), cuneus ($X_{max} = 0$, $Y_{max} = -82$, $Z_{max} = 24$, $z_{max} = -4.244$, nVOX = 354), ventromedial prefrontal cortex ($X_{max} = -2$, $Y_{max} = 50$, $Z_{max} = -8$, $z_{max} = -4.573$, nVOX = 218), precuneus ($X_{max} = -8$, $Y_{max} = -60$, $Z_{max} = 10$, $z_{max} = -5.336$, nVOX = 1221), and posterior cingulate ($X_{max} = 12$, $Y_{max} = -50$, $Z_{max} = 30$, $z_{max} = -5.640$, nVOX = 1311), which, together, correspond to the so-called 'default mode' network identified in resting state fMRI studies (De Luca *et al*, 2006) (Figure 3a). In each of these regions, *decreased* BOLD response during performance of the RVIP task was associated with *heightened* α power.

Effects of nicotine replacement on RVIP-related activity. Our primary hypothesis was that nicotine replacement during short-term smoking cessation would increase activity in ROIs showing α-correlated activation during the RVIP task (ie caudate, dorsal anterior cingulate, dorsolateral prefrontal cortex, insula, parietal lobule, and thalamus). To test this, we entered the mean α-correlated BOLD signal change for the RVIP–CNTRL contrast from these regions into a 2×6 repeated measures ANOVA, with treatment (nicotine *vs* placebo) and ROI as independent variables. We used bilateral ROIs since the regions identified in the RVIP analysis above were bilateral. The results showed significant main effects of treatment ($F(1,14) = 6.09$; $P < 0.05$) and ROI ($F(1,14) = 6.70$; $P < 0.01$). Importantly, there was no significant interaction between the two ($F(1,14) = 1.41$; $P > 0.20$). Confirming our first hypothesis, α-correlated activation was significantly increased by nicotine compared with placebo (mean percent signal change = 0.577 and 0.405, respectively) across these regions. For completeness, we also carried out *post hoc* paired *t*-tests, which confirmed that α-correlated activation was significantly increased by nicotine within each of these ROIs (all $P < 0.05$) except the parietal lobule ($P > 0.2$). Figure 3b shows the mean signal change for the RVIP–CNTRL contrast in each region.

A related hypothesis was that nicotine replacement would further reduce activity in regions showing α-correlated deactivation during RVIP performance (ie angular gyrus, cuneus, precuneus, posterior cingulate, and ventromedial prefrontal cortex). We tested this hypothesis by entering the mean α-correlated BOLD signal change for the RVIP–CNTRL contrast from the bilateral ROIs into a 2×5 repeated measures ANOVA, with treatment and ROI as independent variables. The results showed significant main effects of treatment ($F(1,14) = 8.43$; $P < 0.02$) and ROI ($F(1,14) = 11.06$; $P < 0.005$), but no significant interaction between the two ($F(1,14) = 1.41$; $P > 0.20$). Confirming our second hypothesis, α-correlated deactivations in these regions were further reduced by nicotine relative to placebo (mean percent signal change = −0.572 and −0.364, respectively). *Post hoc* paired *t*-tests confirmed that this effect was significant in each of these regions (all $P < 0.05$) except the

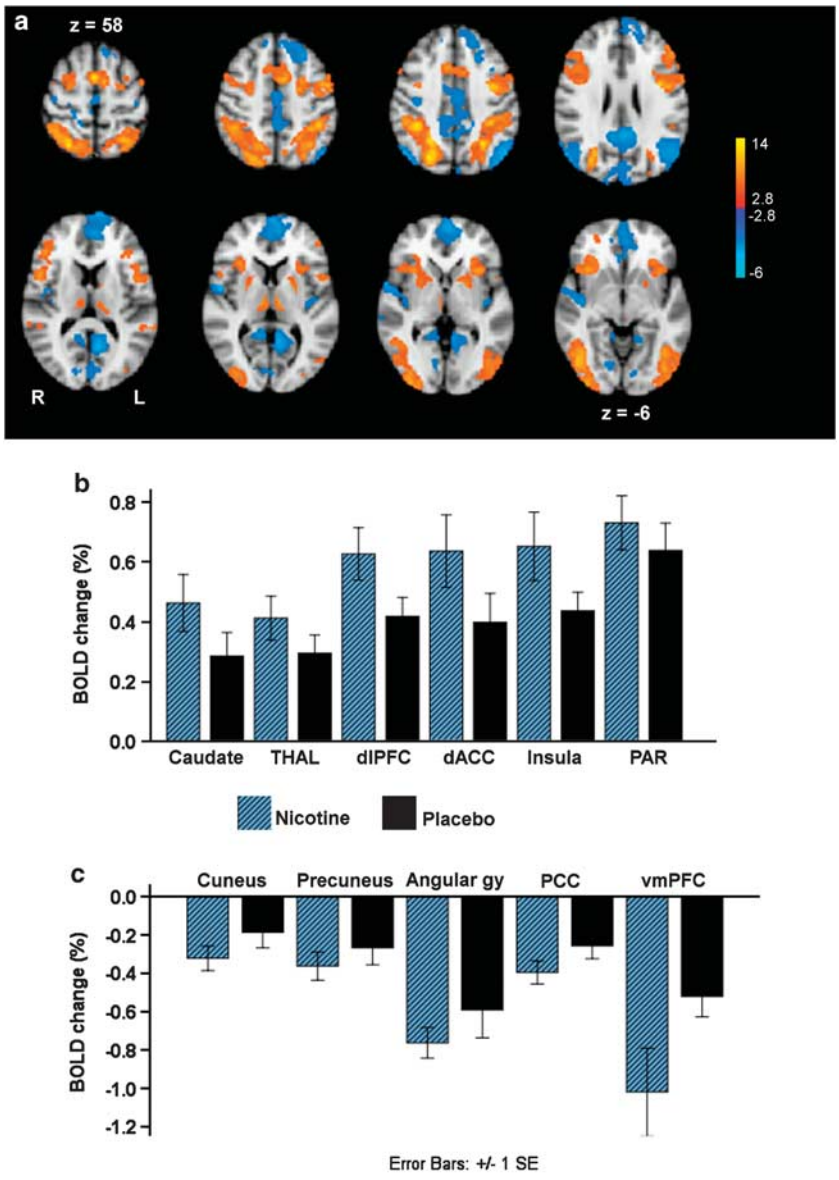

Figure 3 Brain regions of α-correlated activation and deactivation during RVIP performance. (a) Orange/yellow depicts regions of α-correlated activation for the RVIP–CNTRL contrast. Blue depicts regions of α-correlated deactivation for the RVIP–CNTRL contrast. Group analyses were carried out using a mixed-effects analysis with a corrected maximum height threshold of $P<0.005$. (b, c) Mean (+SEM) normalized % BOLD signal change for the contrast RVIP–CNTRL in each ROI at each visit ($N=15$). Angular gy, angular gyrus; dACC, dorsal anterior cingulate cortex; dlPFC, dorsolateral prefrontal cortex; PAR, parietal cortex; PCC, posterior cingulate cortex; THAL, thalamus; vmPFC, ventromedial prefrontal cortex.

precuneus, in which a trend was observed ($P<0.09$). For each region of deactivation, the mean signal change for the RVIP–CNTRL contrast is presented in Figure 3c.

DISCUSSION

We used fMRI with simultaneous EEG recording to investigate changes in brain activity related to cognitive enhancement by nicotine replacement therapy during short-term smoking withdrawal. We found that nicotine replacement was associated with reduced subjective experience of withdrawal symptoms (as assessed by the MMWS) and improved target identification during performance of a demanding RVIP task, consistent with previous behavioral findings (Atzori *et al*, 2008). At the level of neural networks, we found negative correlations between task-related BOLD *increases* and EEG α power in the thalamus, caudate, anterior insula, parietal lobule, dorsal ACC, and DLPFC. In support of our primary hypothesis, nicotine replacement during smoking withdrawal potentiated the α-correlated BOLD activity in each of these regions, except parietal lobule. We also found negative correlations between task-induced BOLD *decreases* (ie, task-related deactivation) and EEG α power in regions comprising the 'default mode' network (including the posterior cingulate, precuneus, angular gyrus, and ventromedial prefrontal cortex (De Luca *et al*, 2006). Nicotine replacement also potentiated these α-correlated deactivations,

showing that nicotine suppresses markers of a 'resting' state, consistent with greater task-specific attention (Hahn *et al*, 2007). Together, these results demonstrate that relevant brain networks subserving cognition and attention are pharmacologically modulated directly by nicotine replacement after smoking cessation. These findings provide a neurobiological rationale for use of nicotine replacement to manage cognitive symptoms of smoking cessation in habitual smokers.

We integrated fMRI with EEG to increase confidence that BOLD changes arose from modulation of neuronal activity, rather than from direct effects on vascular response (Iannetti and Wise, 2007; Matthews *et al*, 2006). To our knowledge this is the first pharmacological fMRI study to employ concurrent recording of EEG. This approach is particularly important for fMRI studies of nicotine, which has well-known sympathomimetic properties (Perkins *et al*, 2004; Yugar-Toledo *et al*, 2005) and can have direct effects on neurovascular coupling (Toda, 1975; Boyajian and Otis, 2000; Sabha *et al*, 2000). EEG α power fluctuations provide an electrophysiological index of rhythmic changes in the relative level of depolarization in somatic and dendritic membrane potentials of masses of neurons (Klimesch *et al*, 2007). Although fMRI has high spatial resolution, the BOLD signal has only an indirect relationship with neuronal activity. Scalp EEG on the other hand lacks the spatial resolution of fMRI, but provides a more direct, electrophysiological index of underlying neuronal activity. Because these two imaging modalities provide complementary data, their combination affords a stronger basis for interpreting nicotine's effects on the BOLD response in neuronal terms. In accordance with the present findings, previous research has shown that performance of demanding cognitive tasks is associated with reduced power in the EEG α frequency band, and nicotine administration in abstinent smokers has been shown to reduce α power (Domino *et al*, 2009). At the neuronal level, low α power reflects states of relatively high excitatory activity (Klimesch *et al*, 2007), and in line with the current findings previous simultaneous fMRI–EEG studies have reported negative correlations between α power and spontaneous fluctuations in BOLD activity in frontal, parietal, and thalamic regions (Goldman *et al*, 2002; Laufs *et al*, 2003; De Munck *et al*, 2009).

In the context of demonstrable performance effects of nicotine replacement, the close temporal correspondence between the BOLD and electrophysiological signals provides strong evidence that the improvements in behavior observed here are related to neuronal sources common to the EEG and fMRI signals. Evidence from neurophysiology studies across a number of species including non-human primates suggests that the neuronal processes that give rise to local field potentials are a likely common factor between these two modalities (Goense and Logothetis, 2008; Kayser *et al*, 2004; Logothetis *et al*, 2001). Although fMRI provides localization of the underlying neuronal sources with greater functional anatomical precision than is possible with EEG alone (Goldman *et al*, 2000, 2002; Laufs *et al*, 2003), the fMRI signal does not distinguish between regions that are modulated directly and those that show neuronal activity changes through secondary afferent activity (Schwarz *et al*, 2004). It is important to note that the present approach to integrating fMRI and EEG data is not an attempt to identify the neural generators of the EEG α signal *per se*.

Not all brain regions showing task-specific modulation showed increased activation after nicotine replacement. Although nicotine is associated with excitation post-synaptically, nicotine enhances both glutamatergic and GABAergic pathways pre-synaptically (Mansvelder *et al*, 2002). For example, nicotinic acetylcholine receptors located on GABAergic interneurons known to inhibit pyramidal neurons may provide one pathway via which nicotine can influence network oscillations. Our observations do not allow us to distinguish between nicotine replacement's effects on neuronal excitation or inhibition *per se*. Rather, they more generally support the conclusion that the effects of nicotine replacement on cognitive task performance in smokers are associated with localized changes in the relative balance between excitatory and inhibitory activity.

Previous functional imaging investigations in smokers and non-smokers have reported patterns of modulation involving both activation and deactivation following nicotine administration (Hahn *et al*, 2007, 2009; Lawrence *et al*, 2002; Sweet *et al*, 2010; Thiel *et al*, 2005; Vossel *et al*, 2007). Here, we have built on observations in this study and in previous work to distinguish two large classes of response. We found increased activity in regions known to be involved in sustained attention, executive control and working memory, and decreased activity in brain regions constituting the default mode network. Increased task-related activations in the caudate and thalamus are generally in accord with Lawrence *et al* (2002), who observed a similar pattern of results during RVIP performance following nicotine replacement in non-abstinent smokers (see below for discussion of differences). Our finding that nicotine further reduced task-related deactivations in regions comprising the default network is compatible with several more recent studies of nicotine replacement in non-abstinent smokers (Hahn *et al*, 2007, 2009). What our study uniquely contributes is the integration of these findings in the clinically important context of abstinent smokers after short-term nicotine withdrawal.

We also found that nicotine replacement increased RVIP-related activity in dorsolateral prefrontal and dorsal anterior cingulate regions but not in the parietal lobule, which is in contrast to Lawrence *et al* (2002). The dorsolateral prefrontal cortex has a key role in working memory and executive function (Procyk and Goldman-Rakic, 2006), mediated in part through direct anatomical connectivity with the dorsal anterior cingulate and medial thalamus (Behrens *et al*, 2003; Carter and van Veen, 2007). One potential explanation for the differences between our findings and those of Lawrence *et al* (2002) may be that sensitivity to the effects of nicotine on this functional network may have been increased in our study because we restricted our analysis to regions where task-related activity was significantly correlated with EEG α power. This explanation is congruent with evidence, suggesting that the thalamus may be the central generator of α waves (Klimesch *et al*, 2007) or they may arise from dendritic fields of pyramidal cells in the cortex that receive inputs from subcortical relays including the thalamus and caudate (Bollimunta *et al*, 2008). A second possibility may be that even subtle task differences may elicit different patterns of neural modulation (Hahn *et al*, 2009). Finally, a third

possibility may be that our participants were abstinent for 8 h prior to treatment, whereas most previous functional imaging studies of nicotine's effect on cognition in smokers administered treatment prior to withdrawal onset. However, this latter explanation seems unlikely as one such recent study reported significant nicotine-induced increases in dorsolateral prefrontal cortex activity during performance of an attention task (Hahn *et al*, 2007).

The present findings demonstrate that, relative to placebo, nicotine replacement improves cognitive performance and modulates cognition-related brain activity in deprived smokers, consistent with the results from previous behavioral studies (Atzori *et al*, 2008). However, the question of whether nicotine enhances cognition or remediates a performance deficit remains a topic of debate, with some studies reporting deleterious effects of nicotine on cognition in healthy, non-smokers (Levin *et al*, 2006; Mansvelder *et al*, 2006; Newhouse *et al*, 2004). Nevertheless, results from several previous functional imaging studies suggest that at least under some conditions (eg, low doses) nicotine administration in healthy, non-smokers may improve cognitive performance and modulate task-related brain activity in a number of the same regions found in the current study, including anterior cingulate and superior frontal cortex (Kumari *et al*, 2003; Vossel *et al*, 2007).

In conclusion, our results show that nicotine replacement during short-term smoking withdrawal enhances cognitive task performance and increases related brain activity in regions previously implicated in attention, executive control, and working memory, as well as decreases brain activity in regions of the default network. The close temporal correspondence between the BOLD fMRI and EEG signals across all of these regions lends confidence that these effects reflect the modulation of neuronal activity by nicotine, rather than non-neuronal effects of nicotine on cerebral blood flow or neurovascular coupling. Our findings, therefore, demonstrate that nicotine replacement ameliorates a negative cognitive symptom of smoking withdrawal and modulates brain cognitive networks, in addition to the well-described effects to reduce withdrawal-related nicotine craving (Shiffman *et al*, 2003).

ACKNOWLEDGEMENTS

We thank Ruth Hopper, Sabrina Kapur, Helen Carr, Mark Tanner, Ros Gordon, Graham Lewington, and the clinical team at the GlaxoSmithKline (GSK) Clinical Imaging Centre for help with volunteer recruitment and data collection. We also thank Alex de Crespigny for physics support.

DISCLOSURE

This research was funded by GlaxoSmithKline, which manufactures NiQuitin CQ. All authors were employees of GlaxoSmithKline and JDB, CJL, MJD, LCB, RGM, and PMM owned shares in GlaxoSmithKline at the time the research was conducted. PMM additionally is a part-time employee of Imperial College, London and has received attendance fees for committee work from the Medical Research Council and the Higher Education Funding Council for England. PMM is on the Editorial Board of Nature Reviews Neurology and an Associate Editor of the Journal of Alzheimer's Disease.

REFERENCES

Allen PJ, Josephs O, Turner R (2000). A method for removing imaging artifact from continuous EEG recorded during functional MRI. *NeuroImage* **12**: 230–239.

Allen PJ, Polizzi G, Krakow K, Fish DR, Lemieux L (1998). Identification of EEG events in the MR scanner: the problem of pulse artifact and a method for its subtraction. *NeuroImage* **8**: 229–239.

Atzori G, Lemmonds CA, Kotler ML, Durcan MJ, Boyle J (2008). Efficacy of a nicotine (4 mg)-containing lozenge on the cognitive impairment of nicotine withdrawal. *J Clin Psychopharmacol* **28**: 667–674.

Behrens TEJ, Johansen-Berg H, Woolrich MW, Smith SM, Wheeler-Kingshott CAM, Boulby PA *et al* (2003). Non-invasive mapping of connections between human thalamus and cortex using diffusion imaging. *Nat Neurosci* **6**: 750–757.

Bollimunta A, Chen Y, Schroeder CE, Ding M (2008). Neuronal mechanisms of cortical alpha oscillations in awake-behaving macaques. *J Neurosci* **28**: 9976–9988.

Boyajian RA, Otis SM (2000). Acute effects of smoking on human cerebral blood flow: a transcranial Doppler ultrasonography study. *J Neuroimaging* **10**: 204–208.

Carter CS, Van Veen V (2007). Anterior cingulate cortex and conflict detection: an update of theory and data. *Cogn Affect Behav Neurosci* **7**: 367–379.

De Luca M, Beckmann CF, De Stefano N, Matthews PM, Smith SM (2006). fMRI resting state networks define distinct modes of long-distance interactions in the human brain. *NeuroImage* **29**: 1359–1367.

De Munck JC, Gonçalves SI, Mammoliti R, Heethaar RM, Lopes da Silva FH (2009). Interactions between different EEG frequency bands and their effect on alpha-fMRI correlations. *NeuroImage* **47**: 69–76.

Domino EF, Ni L, Thompson M, Zhang H, Shikata H, Fukai H *et al* (2009). Tobacco smoking produces widespread dominant brain wave alpha frequency increases. *Int J Psychophysiol* **74**: 192–198.

Goense JBM, Logothetis NK (2008). Neurophysiology of the BOLD fMRI signal in awake Monkeys. *Curr Biol* **18**: 631–640.

Goldman RI, Stern JM, Engel J, Cohen MS (2000). Acquiring simultaneous EEG and functional MRI. *Clin Neurophysiol* **111**: 1974–1980.

Goldman RI, Stern JM, Engel JJ, Cohen MS (2002). Simultaneous EEG and fMRI of the alpha rhythm. *NeuroReport* **13**: 2487–2492.

Hahn B, Ross TJ, Wolkenberg FA, Shakleya DM, Huestis MA, Stein EA (2009). Performance effects of nicotine during selective attention, divided attention, and simple stimulus detection: an fMRI study. *Cerebral Cortex* **19**: 1990–2000.

Hahn B, Ross TJ, Yang Y, Kim I, Huestis MA, Stein EA (2007). Nicotine enhances visuospatial attention by deactivating areas of the resting brain default network. *J Neurosci* **27**: 3477–3489.

Heatherton TF, Kozlowski LT, Frecker RC, Fagerström KO (1991). The Fagerström test for nicotine dependence: a revision of the Fagerström tolerance questionnaire. *Br J Addict* **86**: 1119–1127.

Hughes JR, Hatsukami D (1986). Signs and symptoms of tobacco withdrawal. *Arch Gen Psychiatry* **43**: 289–294.

Hughes JR, Peters EN, Naud S (2008). Relapse to smoking after 1 year of abstinence: a meta-analysis. *Addict Behav* **33**: 1516–1520.

Iannetti GD, Wise RG (2007). BOLD functional MRI in disease and pharmacological studies: room for improvement? *Magn Reson Imaging* **25**: 978–988.

Iida M, Iida H, Dohi S, Takenaka M, Fujiwara H, Traystman RJ (1998). Mechanisms underlying cerebrovascular effects of cigarette smoking in rats *in vivo* ò editorial comment. *Stroke* **29**: 1656–1665.

Kayser C, Kim M, Ugurbil K, Kim DS, Konig P (2004). A comparison of hemodynamic and neural responses in cat visual cortex using complex stimuli. *Cerebral Cortex* **14**: 881–891.

Klimesch W, Sauseng P, Hanslmayr S (2007). EEG alpha oscillations: the inhibition-timing hypothesis. *Brain Res Rev* **53**: 63–88.

Kumari V, Gray JA, Ffytche DH, Mitterschiffthaler MT, Das M, Zachariah E *et al* (2003). Cognitive effects of nicotine in humans: an fMRI study. *NeuroImage* **19**: 1002–1013.

Laufs H, Kleinschmidt A, Beyerle A, Eger E, Salek-Haddadi A, Preibisch C *et al* (2003). EEG-correlated fMRI of human alpha activity. *NeuroImage* **19**: 1463–1476.

Lawrence NS, Ross TJ, Stein EA (2002). Cognitive mechanisms of nicotine on visual attention. *Neuron* **36**: 539–548.

Levin ED, McClernon FJ, Rezvani AH (2006). Nicotinic effects on cognitive function: behavioral characterization, pharmacological specification, and anatomic localization. *Psychopharmacology* **184**: 523–539.

Logothetis NK, Pauls J, Augath M, Trinath T, Oeltermann A (2001). Neurophysiological investigation of the basis of the fMRI signal. *Nature* **412**: 150–157.

Mansvelder H, van Aerde K, Couey J, Brussaard A (2006). Nicotinic modulation of neuronal networks: from receptors to cognition. *Psychopharmacology* **184**: 292–305.

Mansvelder HD, Keath JR, McGehee DS (2002). Synaptic mechanisms underlie nicotine-induced excitability of brain reward areas. *Neuron* **33**: 905–919.

Matthews PM, Honey GD, Bullmore ET (2006). Applications of fMRI in translational medicine and clinical practice. *Nat Rev Neurosci* **7**: 732–744.

Newhouse PA, Potter A, Singh A (2004). Effects of nicotinic stimulation on cognitive performance. *Curr Opin Pharmacol* **4**: 36–46.

Ogawa S, Lee TM, Kay AR, Tank DW (1990). Brain magnetic resonance imaging with contrast dependent on blood oxygenation. *Proc Natl Acad Sci* **87**: 9868–9872.

Parrott AC, Garnham NJ, Wesnes K, Pincock C (1996). Cigarette smoking and abstinence: comparative effects upon cognitive task performance and mood state over 24 h. *Human Psychopharmacol Clin Exp* **11**: 391–400.

Parrott AC, Roberts G (1991). Smoking deprivation and cigarette reinstatement: effects upon visual attention. *J Psychopharmacol* **5**: 404–409.

Perkins KA, Lerman C, Keenan J, Fonte C, Coddington S (2004). Rate of nicotine onset from nicotine replacement therapy and acute responses in smokers. *Nicotine Tob Res* **6**: 501–507.

Procyk E, Goldman-Rakic PS (2006). Modulation of dorsolateral prefrontal delay activity during self-organized behavior. *J Neurosci* **26**: 11313–11323.

Royal College of Physicians (2007). Harm reduction in nicotine addiction: helping people who can't quit. *A Report by the Tobacco Advisory Group of the Royal College of Physicians*. London: RCP.

Sabha M, Tanus-Santos JE, Toledo JCY, Cittadino M, Rocha JC, Moreno H (2000). Transdermal nicotine mimics the smoking-induced endothelial dysfunction[ast]. *Clin Pharmacol Ther* **68**: 167–174.

Schwarz AJ, Zocchi A, Reese T, Gozzi A, Garzotti M, Varnier G *et al* (2004). Concurrent pharmacological MRI and *in situ* microdialysis of cocaine reveal a complex relationship between the central hemodynamic response and local dopamine concentration. *NeuroImage* **23**: 296–304.

Shiffman S, Shadel WG, Niaura R, Khayrallah MA, Jorenby DE, Ryan CF *et al* (2003). Efficacy of acute administration of nicotine gum in relief of cue-provoked cigarette craving. *Psychopharmacology* **166**: 343–350.

Smith SM (2004). Overview of fMRI analysis. *Br J Radiol* **77**: S167–S175.

Sweet LH, Mulligan RC, Finnerty CE, Jerskey BA, David SP, Cohen RA *et al* (2010). Effects of nicotine withdrawal on verbal working memory and associated brain response. *Psychiatry Res Neuroimaging* **183**: 69–74.

Toda N (1975). Nicotine-induced relaxation in isolated canine cerebral arteries. *J Pharmacol Exp Ther* **193**: 376–384.

Thiel CM, Zilles K, Fink GR (2005). Nicotine modulates reorienting of visuospatial attention and neural activity in human parietal cortex. *Neuropsychopharmacology* **30**: 810–820.

Vossel S, Thiel CM, Fink GR (2007). Behavioral and neural effects of nicotine on visuospatial attentional reorienting in non-smoking subjects. *Neuropsychopharmacology* **33**: 731–738.

Woolrich MW, Beckmann CF, Nichols TE, Smith SM (2009). Statistical analysis of fMRI data. In: Filippi M (ed). *fMRI Techniques and Protocols* 41, pp 179–236.

Yugar-Toledo JC, Ferreira-Melo SE, Sabha M, Nogueira EA, Coelho OR, Consoline Colombo FM *et al* (2005). Blood pressure circadian rhythm and endothelial function in heavy smokers: acute effects of transdermal nicotine. *J Clin Hypertens* **7**: 721–728.

Supplementary Information accompanies the paper on the Neuropsychopharmacology website (http://www.nature.com/npp)